Evaluating the Microstructure of Photoluminescent Concrete Pavement Containing Strontium-Aluminate, Acrylic and Recycled Waste Glass

Maqsud, A. S., Amin, S. & Iqbal, R.

Original citation:
Maqsud, AS, Amin, S & Iqbal, R 2021, 'Evaluating the Microstructure of Photoluminescent Concrete Pavement Containing Strontium-Aluminate, Acrylic and Recycled Waste Glass', IOP Conference Series: Materials Science and Engineering, vol. 1196.
https://dx.doi.org/10.1088/1757-899X/1196/1/012020

DOI 10.1088/1757-899X/1196/1/012020
ISSN 1757-8981
ESSN 1757-899X

Publisher: IOP Publishing

Evaluating the Microstructure of Photoluminescent Concrete Pavement Containing Strontium-Aluminate, Acrylic and Recycled Waste Glass

Evaluating the Microstructure of Photoluminescent Concrete Pavement Containing Strontium-Aluminate, Acrylic and Recycled Waste Glass

Ahmed Seyab Maqsud[1], **Shohel Amin**[1*] **and Rahat Iqbal**[2]

[1]Energy, Construction Environment, Coventry University, Priory Street, Coventry CV15FB, UK
[2] Interactive Coventry Ltd., Coventry University Technology Park, Puma Way, Coventry, CV1 2TT, UK
* **E-mail:** Shohel.Amin@coventry.ac.uk

Abstract. This paper constructs the photoluminescent concrete pavement (PhotoCP) mixing the photoluminescent material (Strontium-Aluminate) with recycled waste glass and transparent acrylic to visible the neighbourhood streets without streetlights. The non-destructive analyses of photoluminescent materials were conducted using the X-Ray Fluorescence, X-Ray diffraction, and Scanning Electron Microscopy instruments to understand the behaviour of atoms in photoluminescent materials when they interact with radiation. The compressive strength test examined the load bearing capacity of PhotoCP. A 30cm x 230cm test bed was constructed at a neighbourhood street in Peshawar, Pakistan to assess the impact of photoluminescent materials on lighting the neighbourhood street. The non-destructive analyses and compressive strength test show that PCP specimens have good interlocking capability, structural strength and durability. The testbed experiment observed the illuminance of PhotoCP for a period of 6 to 8 hours with highest lumen intensity of 1-3 lux from sunset to 8:30 pm.

Keywords: Strontium Aluminate, RWG, XRF, XRD, SEM image, compressive strength.

1. Introduction

The electricity costs for street lighting are a significant expenditure for municipalities. There is a substantial increase in the electricity cost around the world particularly through the rapid increase in the cost of oil and gas [1]. For promoting energy efficiency streetlighting, studies focused on the consumption, production patterns and program costs of streetlights minimising the electricity consumption [2-3]. To achieve the short-term energy efficiency of urban streetlighting, municipalities sometimes adopt a 'part-night' lighting system particularly in the residential areas where lights of relatively lower importance (in respect of traffic accident and crime rate) are dimmed or switched off at times during the night when they are least likely to be needed [1,4]. The energy efficient streetlights and 'part-night' lighting system reduce the energy consumption and carbon emission; however, the municipalities are still struggling to light up the urban streets due to budget deficit leaving many urban streets in dark in developing countries. The luminescent road marks can ensure safety and security at urban access roads where traffic volume at night is low.

The photoluminescence phenomenon of pavement materials can be a source of road illumination at night by constructing the road surface with phosphorescent materials. Strontium-Aluminate is a

photoluminescent material that is white, nontoxic and non-radioactive powder commonly used in artistic or decorative purposes. The slower time-scale emission of light from the Strontium-Aluminate ($SrAl_2O_4$), transition from 4f to 5d of the Europium (Eu^{2+}), make it a good candidate for the phosphorescent road material [5]. Several studies discuss on the emission intensity and luminescence capacity of Strontium-Aluminate [5-10]. Bone [6] partially substituted the Calcium (Ca^{2+}) and Strontium (Sr^{2+}) sites in the matrix for enhancing the emission intensity and luminescence of $SrAl_2O_4$ with Eu^{2+} and Dysprosium (Dy^{3+}). Similarly, Katsumata et al. [5] investigated the phosphorescence characteristics of $Sr_3Al_2O_6$, $SrAl_2O_4$, $SrAl_4O_7$, and $SrAl_{12}O_{19}$ polycrystalline ceramic doped with Eu^{2+} and Dy^{3+}. Luitel et al. [8] examined the Eu^{2+} and Dy^{3+} doped phosphors and illustrated the causes of higher brightness and slow-scale light emission from the Dy^{3+} doped phosphors comparing to Eu^{2+} doped phosphors. Praticò et al. [10] experimented the photoluminescent phenomenon of dense-graded and open-graded friction courses and the surface modifications (friction and texture) due to the coating of photoluminescent material.

This paper constructs the photoluminescent concrete pavement mixing the photoluminescent material (Strontium-Aluminate) with recycled waste glass (RWG) and transparent Acrylic to visible the neighbourhood streets without the streetlights. The RWG is widely used in glass–ceramics, tiles for flooring or lining, foam glass and insulating or reinforcing fibre [11]. There are some evidences of using the RWG in the concrete pavements [12-14], however this study, for the first time, applies it in the photoluminescent concrete pavement for refracting the light rays to the Strontium-Aluminate particles. The Acrylic was used as the transparent binder of Strontium-Aluminate and coarse aggregates in the concrete pavement. The glass particles in the concrete refract the daylight as well as the light emission from the Strontium-Aluminate particles. The United Nations estimated that the annual volume of solid waste was 200 million tonnes of which 7% were made up of glass [15]. A test bed was constructed at the neighbourhood street in Peshawar, Pakistan where 113 tons of glass waste is generated daily from municipal waste [16].

2. Materials and Experiments

2.1. Photoluminescent Materials

The strontium aluminate, acrylic and glass powder were mixed with cement and aggregates to manufacture the photoluminescent concrete pavement (Figure 1a and 1b). Acrylic is a transparent thermoplastic (methyl methacrylate) and acts as a transparent binder for the Strontium-Aluminate and coarse aggregates of concrete pavement (Figure 1c and 1d). Acrylic binder resin enhances the stability, photoluminescence and surface absorption of photoluminescent concrete pavement [17]. The glass powder was used in the concrete mixture instead of sand because glass particles refract the ray of light to the Strontium-Aluminate particles enhancing the invisible ultraviolet energy from the natural light source (Figure 1e and 1f). The recycled glass wastes were collected from the local recycle stores and grounded into glass powder. The glass powder was passed through no. 20 sieve.

Three groups of photoluminescent concrete cubes were manufactured mixing cement, glass powder, Strontium-Aluminate and coarse aggregates to understand the significance of Strontium-Aluminate and glass powder on the photoluminescence phenomenon of photoluminescent concrete pavement (Figure 2). Group 1 specimens were designed with 2 inches top layer of cement, glass powder, Strontium-Aluminate and coarse aggregates mixture. The four inches bottom layer was made of cement, glass powder and coarse aggregates (Figure 3). Sand replaced glass powder at the bottom 4 inches layer of Group 2 specimens to understand the impact of glass particles on refracting the light rays (Figure 3). Group 3 specimens are the standard (base) concrete cubes with 1:2:4 ratios of cement, sand and coarse aggregates, respectively (Figure 3).

(a) Cement, Strontium Aluminate, and glass powder (in light)

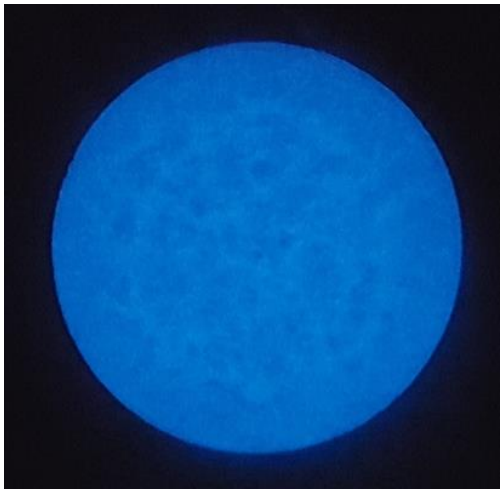

(b) Cement, Strontium Aluminate, and glass powder (in dark)

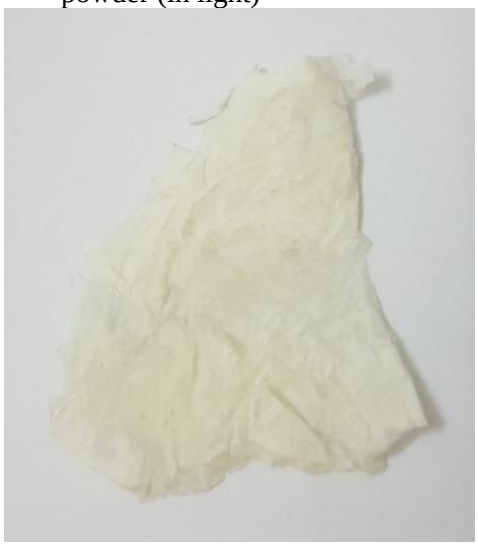

(c) Acrylic mixed with Strontium-Aluminate (in light)

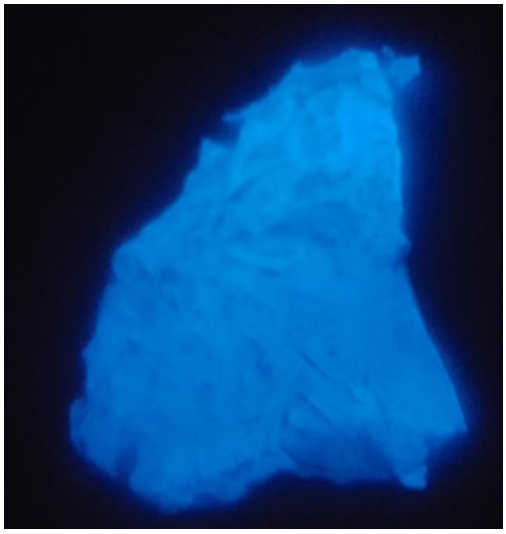

(d) Acrylic mixed with Strontium-Aluminate (in dark)

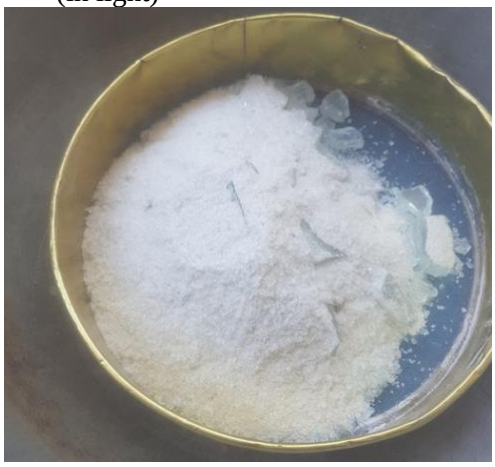

(e) Recycled glass waste powder

(f) Recycled glass powder passed through 20 no. sieve

Figure 1. Photoluminescent materials

Figure 2. Concrete cube samples (6x6x6 in) of three groups

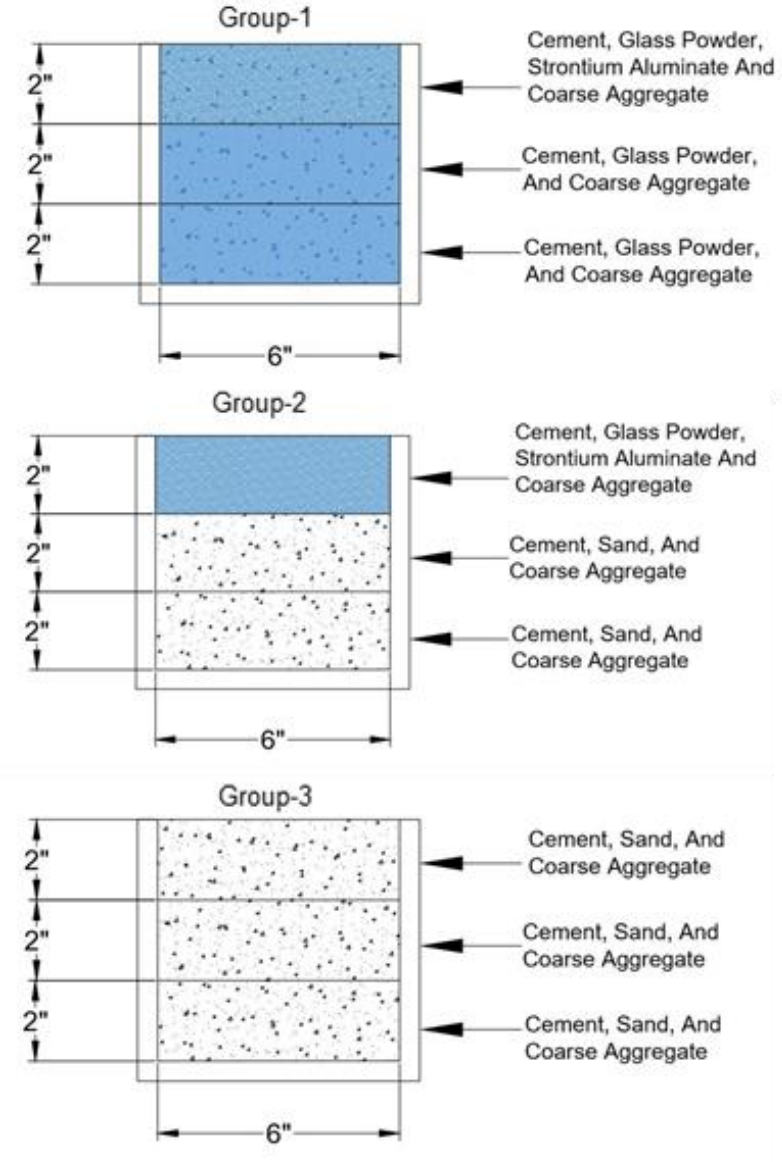

Figure 3. Schematic diagrams of concrete specimens of three groups

2.2. Laboratory experiments

2.2.1 Chemical experiments

The non-destructive analyses of photoluminescent materials were conducted using the X-Ray Fluorescence (XRF), X-Ray diffraction (XRD), and Scanning Electron Microscopy (SEM) instruments to understand the behaviour of atoms in photoluminescent materials when they interact with radiation. XRF analysed the chemical elements in concrete specimens based on the measurement of wavelengths and intensities of their spectral lines emitted [18]. The XRF imaged the cross-section of the concrete specimens and determined the concentrations of Strontium Aluminate and glass particles. X-rays interact weaker with matter than electrons and so they penetrate deeper into the sample.

This deeper penetration makes the results less sensitive to the surface roughness [19]. XRF has comparatively high detection limits due to high background produced by the absorption and scattering of X-ray beam by the sample and matrix [18]. Different calibration plots are required for different matrices to offset the matrix effects. The XRD technique was used to find the crystal structure properties of the Strontium-Aluminate and glass powder determining the average bulk composition. The XRD produces the patterns of peak positions and relative intensities that characterise the crystal structures and enable identifying the presence of Strontium-Aluminate and glass powder in the concrete specimens [20]. The SEM analysed the morphology of Strontium-Aluminate and glass powder and assessed the interlocking spatial variations in chemical compositions of particles. The elongated particles with long edges are prone to air voids and structural disintegrity.

2.2.2 Structural experiments

Several tests such as accelerated pavement testing and plate load test examine the pavement response and modulus of subgrade reaction under the controlled and accelerated accumulation of wheel loads in a compressive time period. Local streets in residential neighbourhood, mostly utilise for leisure and play, have slow speed light traffic, occasional delivery vans and walking and bicycle facilities. Since the neighbourhood streets are not subjected to accelerated accumulation of damage by heavy trucks and the concrete pavements are much stronger in compression than in tension, the compressive strength tests were experimented on the concrete specimens. Moreover, glass powder replaced sand as the filler in the concrete specimens and the durability and deformation of the specimens with glass powder were compared with the controlled specimens (Group 3).

2.3 Testbed at neighbourhood street in Peshawar, Pakistan

A test bed of 1 x 7.5 feet (30 cm x 230 cm) was constructed at the neighbourhood street in Peshawar, Pakistan to understand the impact of photoluminescent materials on lighting the neighbourhood street (Figure 4a). The photoluminescent concrete blocks were cured in the laboratory and placed on the neighbourhood road after for 3 days to avoid hindering the neighbourhood mobility. This neighbourhood street was selected as a testbed because there is no streetlight in this street and the emission rate and duration of light rays from the photoluminescent concrete pavement can be examined after the dawn (Figure 4b).

(a) The photoluminescent concrete blocks were placed after 3 days curing (b) The photoluminescent concrete pavement testbed

Figure 4. Testbed construction at the neighbourhood street in Peshawar Pakistan

3. Experimental Results

3.1 Chemical Experiments

The non-destructive analyses of photoluminescent materials using XRF, XRD and SEM tools produce the controlled populations of point defects and multiple defect clusters such as voids, stacking-fault tetrahedra and dislocation loops [21]. The XRF elemental analysis, independent of the chemical form of the elements, measures the concentration of different elements in the photoluminescent materials by the X-rays intensity that is proportional to the concentration of an element and the strength of the ionizing source [22]. This study applied the fundamental parameter method for quantitative XRF analysis that is based on the primary and secondary radiations to calculate the intensity of analyte radiation in the specimen of known composition [23]. Ten elements were identified in the Strontium-Aluminate materials such as Strontium (Sr), Chlorine (Cl), Calcium (Ca), Manganese (Mn), Dysprosium (Dy), Thulium (Tm), Copper (Cu), Tungsten (W), Rubidium (Rb) and Rhodium (Rh). The Dy^{3+} (1.14%) doped Sr has major contribution (86.62%) in the Strontium-Aluminate (Table 1). The Dy^{3+} doped Strontium-Aluminate has excellent emission characteristics, single luminescent centre and high absorption efficiency in the Ultraviolet region [24]. The Dy^{3+} doped Strontium-Aluminate has higher emission rate comparing to Eu^{2+} phosphor and can emit light 6 to 10 hours at night [8,10].

The recycled glass waste powder consists of Sr, Silicon (Si), Sulfur (S), Rh, Potassium (K), Ca, Titanium (Ti), Chromium (Cr), Mn, Iron (Fe), Cu and Zirconium (Zr). Major constituent of recycled glass waste is quartz (SiO_2) that is also the major constituent of the sand (Table 1). A typical brown sand in concrete application contains up to 80% quartz along with iron, carbonate, potassium and other elements. The recycled glass waste contains 87.31% silica that ensures the stronger binding of concrete mixture (Table 1). The recycled glass powder also contains 23.91% Ca and 11.41% calcium oxide (CaO) (Table 1). The CaO crystallises each other and other substances in the concrete through hydration process and the carbonation process of calcium hydroxide increases the mechanical strength of the concrete and decreases the pH level. There is no toxic element or compound in the recycled glass powder.

The qualitative analysis of XRD data based on relative peak intensities identifies the presence of any impurity phases of composition different from Strontium-Aluminate and glass materials [24]. The XRD data were compared with a known phase diagram available at online databases such as International Centre for Diffraction Data (ICDD) to find unknown minerals [25]. The highest peak in the XRD diffractogram of strontium aluminate is at 30^0 angles on 2Theta axis with a value of 2.98 (Figure 5a). The compound phases of strontium aluminate in the XRD diffractogram are $SrAl_2O_4$ and $SrAl_2O_8Si_2$

while the crystal system and space groups are cubic and monoclinic, and P1211 and Pm-3m, respectively.

The recycled glass waste powder has too many peaks and no sharp diffraction peak because glass is amorphous. Instead of peaks, the rising background is observed in the XRD diffractogram of glass that consists of one or more broad diffuse rings [26]. The intensity curve of recycled glass waste in the XRD diffractogram very closely follow the absolute basis (electron units per SiO_2) (Figure 5b). The compound phase, crystal system and space group of recycled glass waste powder in the XRD diffractogram are SiO_2, hexagonal and P6/mmm.

The XRD pattern of strontium aluminate and glass powders provides data on crystal structure but unable to provide the morphology of the surface [6]. The SEM images observe the surface morphology and crystalline sizes of strontium aluminate and glass powders (Figure 6 and 7). Figure 6 shows that the particles in the strontium aluminate range from sub-micron size to several tens of μm sizes and have well distinct boundaries that provide good interlocking between particles. The strontium aluminate powder has finer and round shaped particles than glass powder but also possesses needle like particles at very small scale ensuring interlocking ability (Figure 6). The interlocked and closely spaced particles in the strontium aluminate powder increase the compressive strength of concrete because the load transfers uniformly from particle to particle down to the subgrade soil.

The SEM images of recycled glass waste powder show that particles are irregular and angular with distinct boundaries which is an indication of good particle interlocking (Figure 7). The particle sizes of glass powder range from 10μm to hundreds of μm with little number of particles in sub-micron size (Figure 7). There are more surface area contacts between the particles in glass powder mitigating the crack development in the concrete. In addition, the irregular and angular shapes of glass powder particles increase the strength of hardened concrete but prejudice the workability of fresh concrete [27]. The XRF and XRD analyses determine the chemical composition and crystal structure of Strontium-Aluminate and recycled glass waste powders arguing the materials purity in the photoluminescent concrete pavement. The SEM analyses conclude that mixture of Strontium-Aluminate and recycled glass waste powders in the concrete will enhance the compressive strength and workability of concrete after assessing the morphological structure of the materials.

3.2 Compressive strength analysis of concrete specimens

The compressive strength tests of 3-group of concrete specimens were conducted to correlate with the flexural strength by calibrating the relationship between flexural and compressive strength in order to check compliance. The compressive strength of Group 1 specimens that included RWG instead of sand reduced by 5.6% in comparison with Group 3 specimens (fine aggregates are sand) (Table 2). The compressive strength of Group 2 specimens was reduced by 22.65% comparing with that of Group 3 specimens (Table 2). The reduction of compressive strength of group 1 and 2 specimens was due to the presence of Strontium-Aluminate materials in the upper 2-inch layer because the SEM images of RWG powder showed the good particle interlocking. The crack developed in the bottom layer (contains sand) of Group 2 specimens during the compression tests justify the above-mentioned argument. The average compressive strengths of target specimens of Group 1 and Group 2 are 3738 psi (25.77 N/mm^2) and 3323.78 psi (22.92 N/mm^2), respectively (Table 2). The recommended minimum compressive strength classes of road pavement (concrete cube) are within the range of C16/20 (20N/mm^2) and C35/45 (40N/mm^2) to achieve suitable durability, regardless of the structural strength requirements. Higher strengths are sometimes used but can lead to higher shrinkage and higher costs. This is usually only justifiable where extreme conditions are present such as highly abrasive operations or where high impact resistance is required. Otherwise the detrimental effects of higher shrinkage usually outweigh any benefits from higher strength. There is also often a drop off in correlation between high compressive strength and flexural strength which leads to diminishing returns.

Table 1. XRF Analysis of Strontium-Aluminate and RWG powder.

	Powder elements			**Powder oxide**		**Element [3-sigma]**		**Oxide [3-sigma]**		**Line**	**Element - Int (cps/uA)**		**Oxide - Int (cps/uA)**	
Analyte	Strontium-Aluminate	Glass	Analyte	Strontium-Aluminate	Glass	Strontium-Aluminate	Glass	Strontium-Aluminate	Glass		Strontium-Aluminate	Glass	Strontium-Aluminate	Glass
Si		73.37 %	SiO_2		87.31 %		[0.788]		[0.937]	SiKa		24.770		24.866
Sr	86.62%	0.06 %	SrO	87.78%	0.02 %	[0.116]	[0.002]	[0.118]	[0.001]	SrKa	11960.139	9.032	11959.416	9.943
Cl	11.64%		Cl	10.39%		[0.346]		[0.304]		ClKa	21.619		22.163	
Dy	1.14%		Dy_2O_3	1.13 %		[0.028]		[0.028]		DyLa	27.263		27.082	
Ca	0.19%	23.91 %	CaO	0.23 %	11.41 %	[0.034]	[0.117]	[0.042]	[0.056]	CaKa	1.331	123.245	1.329	121.307
Fe		1.55 %	Fe_2O_3		0.65 %		[0.011]	[0.008]	[0.005]	FeKa		48.279		49.809
Mn	0.17%	0.04 %	MnO	0.19 %	0.01 %	[0.007]	[0.005]		[0.002]	MnKa	8.649	0.795	8.604	0.837
Rb	0.13%		Rb_2O	0.10 %		[0.007]		[0.007]		RbKa	23.849		19.531	
Tm	0.07%		Tm_2O_3	0.06 %		[0.023]		[0.023]		TmLa	2.307		2.137	
W	0.03%		WO_3	0.02 %		[0.009]		[0.010]		WLa	1.692		0.836	
Cu	0.02%	0.04 %	CuO	0.03 %	0.01 %	[0.004]	[0.003]	[0.004]	[0.001]	CuKa	3.057	2.373	3.322	2.352
S		0.44 %	SO_3		0.40 %		[0.068]		[0.064]	SKa		0.415		0.409
Ti		0.32 %	TiO_2	0.08 %	0.16 %		[0.009]	[0.021]	[0.004]	TiKa		2.618	0.913	2.616
K		0.16 %	Ag_2O		0.02 %		[0.025]		[0.001]	KKa		0.483		2.387
Zr		0.06 %					[0.002]			ZrKa		10.164		
Cr		0.04 %	Cr_2O_3		0.02 %		[0.006]		[0.002]	CrKa		0.650		0.709

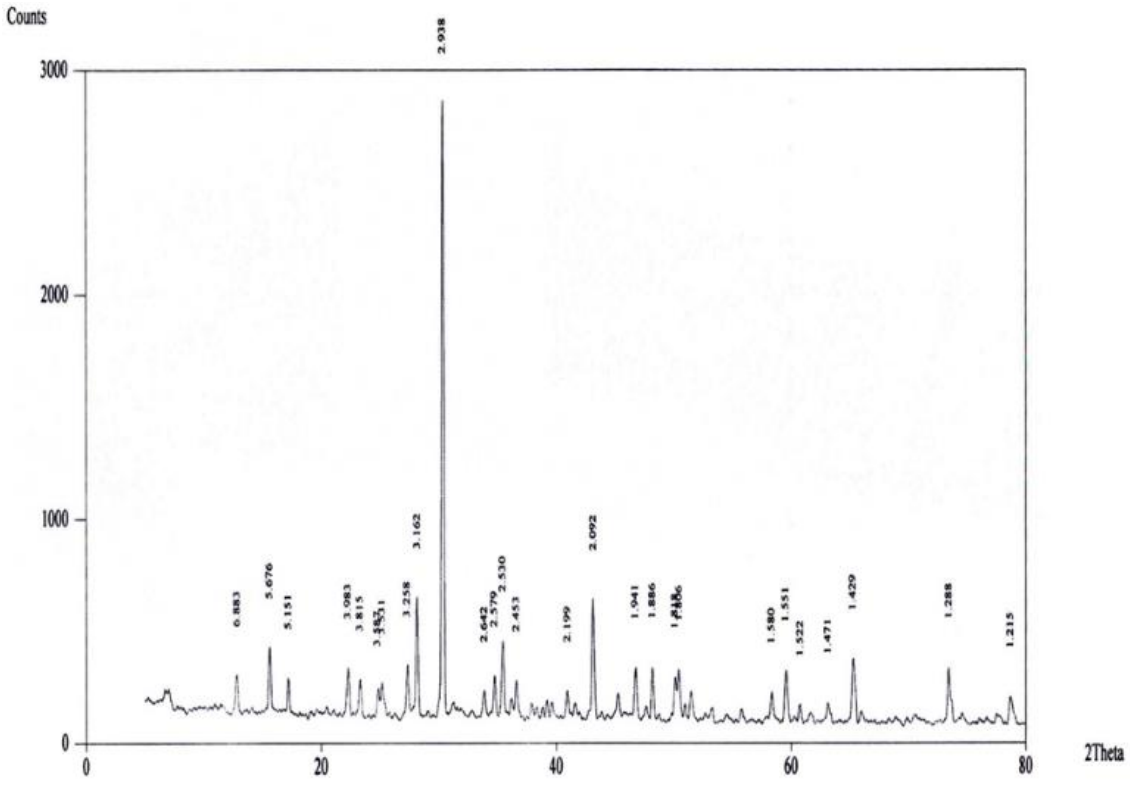

(a) Strontium Aluminate

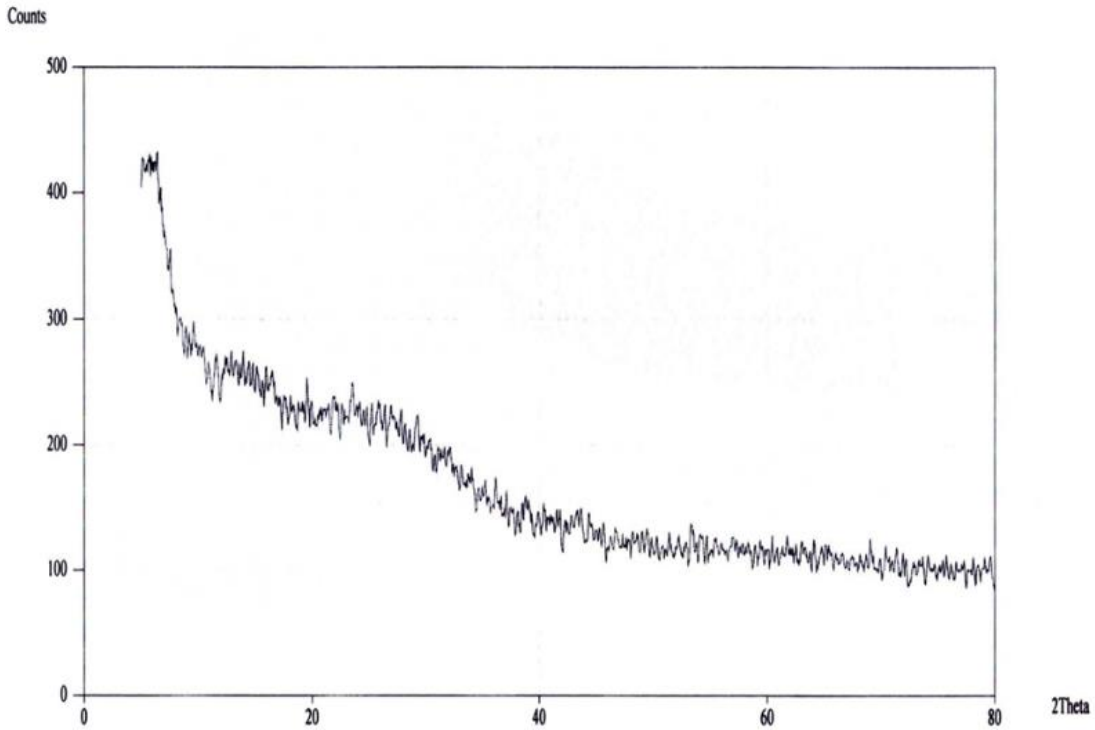

(b) Glass Powder

Figure 5. XRD diffractograms analysis

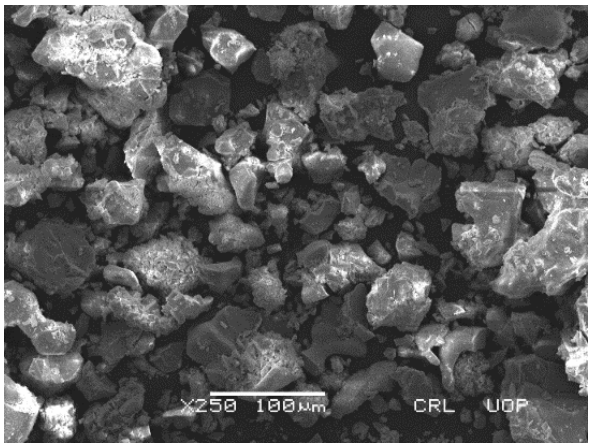

(a) x250 magnification level (100µm)

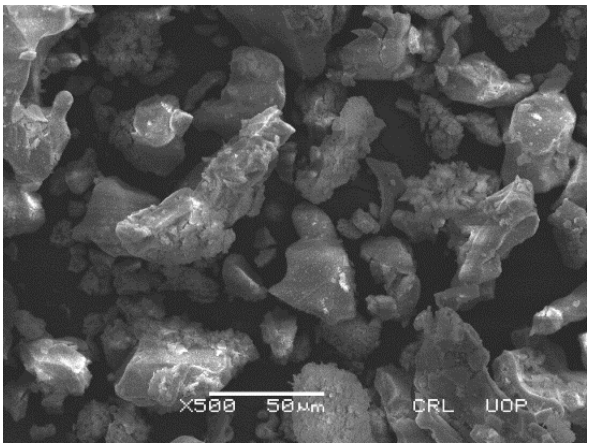

(b) X500 magnification level (50µm)

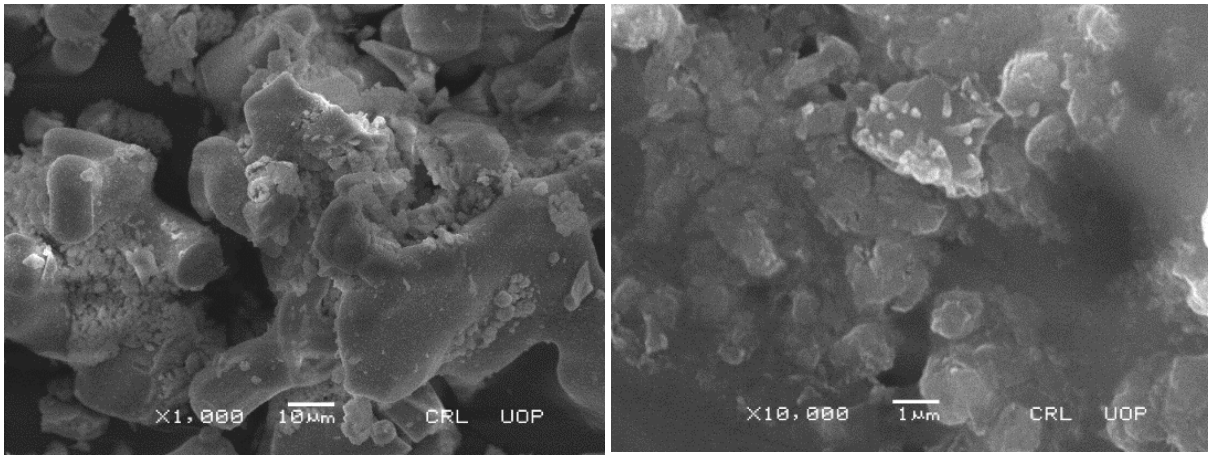

(c) X1000 magnification level (10µm) (d) X10000 magnification level (1µm)

Figure 6. SEM image micrographs of Strontium Aluminate

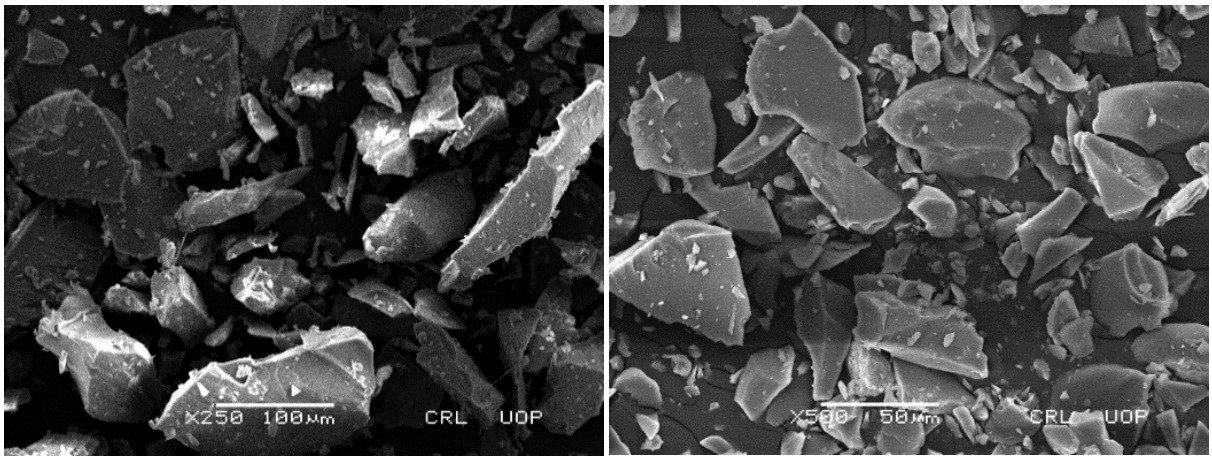

(a) x250 magnification level (100µm) (b) X500 magnification level (50µm)

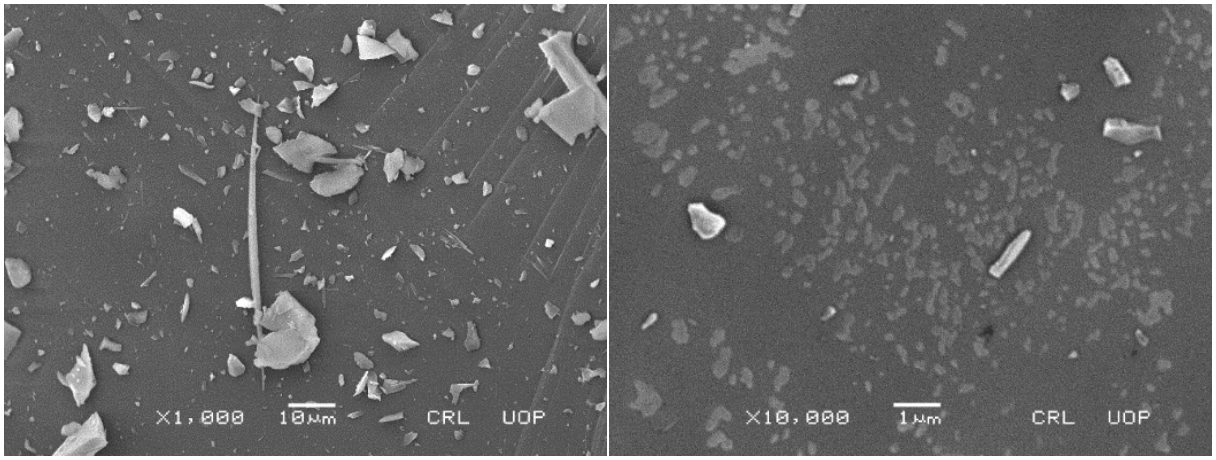

(c) X1000 magnification level (10µm) (d) X10000 magnification level (1µm)

Figure 7. SEM micrographs of recycled glass waste powder.

Table 2. Compression test results of Group 1, 2 and 3 specimens

	Sample No.	Load (tonnes)	Compressive Strength (psi)	Compressive Strength (N/mm^2)	Average compressive Strength (psi)	Average compressive Strength (N/mm^2)
GROUP-1	1	36	3654.95	25.20	3738.11	25.77
	2	38.7	3818.84	26.33		
	3	37.4	3740.52	25.79		
GROUP-2	1	30.5	3317.01	22.87	3323.78	22.92
	2	30.6	3324.26	22.92		
	3	30.7	3330.07	22.96		
GROUP-3	1	39.7	3881.21	26.76	3872.51	26.70
	2	39.6	3873.96	26.71		
	3	39.4	3862.36	26.63		

3.3 Photoluminescent concrete pavement at a neighbourhood street in Peshawar, Pakistan

The illuminance (lumen/m^2), also known as lux, of the photoluminescent concrete pavement was recorded at the testbed in the neighbourhood street from dusk to 9:00 o'clock at night (Figure 8). It was observed that during the time period between dusk to sunset, lux value was within the range of 0.5 to 2. The illuminance of pavement increases after the sunset (approximately 6:30 pm) within the range of 1-3 lux until 8:30 pm. The illuminance started decreasing after 8:30 pm but at deep twilight (approximately 1 lux) condition after two hours. The photoluminescent materials absorbs the light rays from the passing by vehicles and started glowing despite low lux level after 8:30 pm. The emission rate of light ray from the photoluminescent pavement strip was uniform and higher after 3-4 days of placement on the neighbourhood streets. There was no crack or structural damage of the testbed 28 days after the construction. The National Optical Astronomy Observatory recommends the illuminance level for local roads within the range of 3 to 6 lux. The observed illuminance of the 30 cm x 230 cm photoluminescent pavement strip at neighbourhood street was within the lower recommended illuminance level for local roads for a couple of hours after the sunset. The complete construction of neighbourhood cul-de-sac and streets enhances the attractiveness of evening walking, bicycling and social gathering.

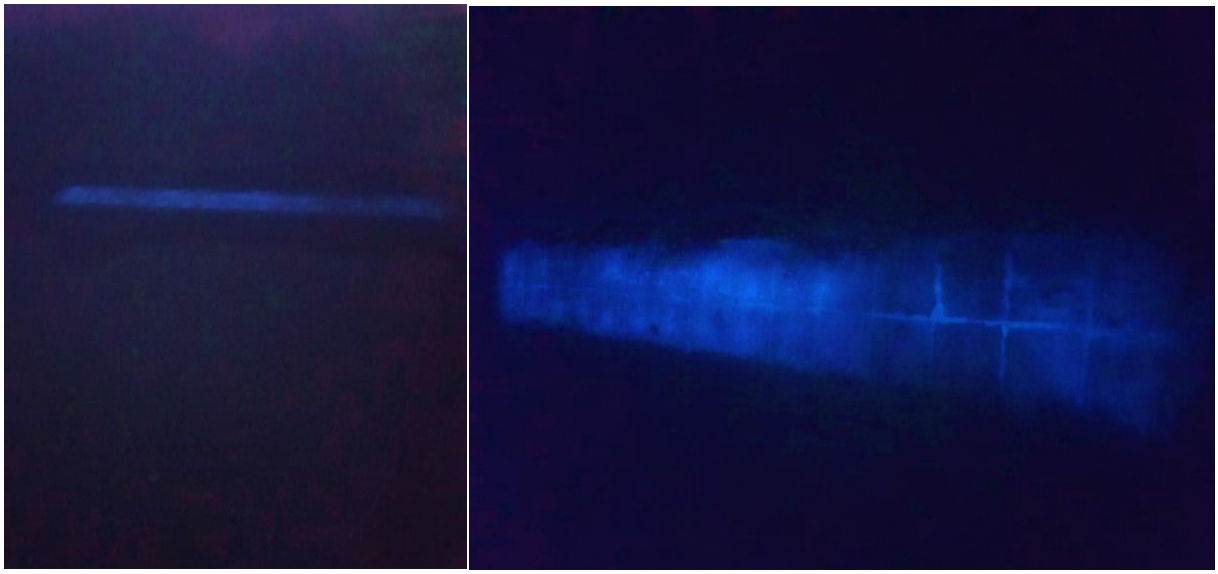

(a) Day 1 (b) Day 2

Figure 8. The illuminance of photoluminescent concrete pavement

4. Conclusions

This study carried out an experiment mixing the Strontium-Aluminate and RWG powders in concrete to manufacture the photoluminescent concrete pavement for the neighbourhood street. The XRF test of Strontium-Aluminate and glass powder identified that Strontium, Chlorine and Dysprosium were the main components of Strontium-Aluminate sample and the Silicon, Calcium and Iron were the main components of RWG power passed through the 20-mesh sieve. The presence of Chlorine (11.64%) in the Strontium-Aluminate sample reduces the potential growth of bacteria and algae on the concrete pavement. The major constituents of Strontium-Aluminate and RWG powders were $SrAl_2O_4$ (85.56%) and SiO_2 (87.31%), respectively. The XRD results of Strontium-Aluminate and RWG powders didn't find any foreign substance justifying the purity of materials. The SEM image micrographs analysed the morphological structure of Strontium-Aluminate and RWG powder. The Strontium-Aluminate particles were rounded and finer shape like clay and had smooth edges, whereas the particles of RWG were irregular with distinct and sharp edges. The SEM images show the good interlocking capability of both materials.

The compressive strength tests of the specimens show the structural strength and durability of photoluminescent concrete cubes. The testbed experiments at the neighbourhood street observed the illuminance of the photoluminescent concrete pavement for a period of 6 to 8 hours with highest level of illuminance from the sunset to 8:30 pm. This study not only utilised the RWG in place of sand in the concrete pavement but also manufactured the energy efficient concrete pavement by mixing the Strontium-Aluminate material. The Strontium-Aluminate powder is usually used in painting and toys, however for the first time this study examined its effectiveness in the photoluminescent concrete pavement and saving the energy cost for streetlighting at the neighbourhood street. This study opens the window for potential study examining the further improvement in the photoluminescent materials and techniques for enhancing the illuminance of photoluminescent concrete pavement that would reduce the energy costs of city councils for streetlighting.

5. References

[1] Pagden M, Ngahane K and Amin M S R (2020). Changing the colour of night on urban streets - LED vs. part-night lighting system. *Socio-Economic Planning Sciences* **69**, 100692. https://doi.org/10.1016/j.seps.2019.02.007

[2] Escolar S, Carretero J, Marinescu M and Chessa S (2014). Estimating Energy Savings In Smart Street Lighting By Using An Adaptive Control System. *International Journal of Distributed Sensor Networks*. **10**(5), 971587. DOI: https://doi.org/10.1155/2014/971587

[3] Iveland J, Martinelli L, Peretti J, Speck J S, and Weisbuch C (2013). Direct measurement of Auger electrons emitted from a semiconductor light-emitting diode under electrical injection: identification of the dominant mechanism for efficiency droop. *Physical review letters*. **110**(17), 177406. DOI: https://doi.org/10.1103/PhysRevLett.110.177406

[4] Plainis S, Murray I J and Pallikaris I G (2006). Road traffic casualties: understanding the night-time death toll. *Injury Prevention.* **12**(2), 125-138. DOI: http://dx.doi.org/10.1136/ip.2005.011056

[5] Katsumata T, Sasajima K, Nabae T, Komuro S and Morikawa T (1998) Characteristics of Strontium-Aluminate crystals used for long-duration phosphors. *Journal of the American Ceramic Society*.

[6] Bone A N (2017). *Optimization of a Strontium-Aluminate* ". Oak Ridge National Lab. (ORNL), Oak Ridge, TN (United States).

[7] Gill R (2014) *Modern Analytical Geochemistry: an introduction to quantitative chemical analysis techniques for Earth, environmental and materials scientists*. Routledge.

[8] Luitel H, Watari T, Chand R, Torikai T and Yada M (2013) Giant Improvement on the Afterglow of Sr4Al14O25:Eu2+,Dy3+ Phosphor by Systematic Investigation on Various Parameters. *Journal of Materials*. 2013, pp.1-10.

[9] Egerton R F (2005) *Physical principles of electron microscopy*. New York: Springer.

[10] Praticò F, Vaiana R and Noto S (2018) Photoluminescent Road Coatings for Open-Graded and Dense-Graded Asphalts: Theoretical and Experimental Investigation. *Journal of Materials in Civil Engineering*. **30**(8), p.04018173.
[11] Colombo P, Brusatin G, Bernardo E and Scarinci G (2003). Inertization and reuse of waste materials by vitrification and fabrication of glass-based products. *Current Opinion in Solid State and Materials Science*. **7**, 225–239. https://doi.org/10.1016/j.cossms.2003.08.002
[12] Arulrajah A, Ali M Y, Disfani M M and Horpibulsuk S (2014). Recycled-Glass Blends in Pavement Base/Subbase Applications: Laboratory and Field Evaluation. *Journal of Materials in Civil Engineering*. **26**(7), 04014025. https://doi.org/10.1061/(ASCE)MT.1943-5533.0000966
[13] Arulrajah A, Piratheepan J, Disfani M M and Bo M W (2013). Geotechnical and geo-environmental properties of recycled construction and demolition materials in pavement subbase applications. *Journal of Materials in Civil Engineering* **25**(8), 1077-1088. https://doi.org/10.1061/(ASCE)MT.1943-5533.0000652
[14] Jamshidi A, Kurumisawa K and Nawa T (2016). Performance of pavements incorporating waste glass: The current state of the art. *Renewable and Sustainable Energy Reviews*. **64**, 211-236. https://doi.org/10.1016/j.rser.2016.06.012
[15] Demir I (2009). Reuse of waste glass in building brick production. Waste Management & Research: *The Journal for a Sustainable Circular Economy*. **27**(6), 572-577. https://doi.org/10.1177/0734242X08096528
[16] International Trade Administration (2018). Pakistan - Waste Management | Export.Gov (2018) [online] available from <https://www.export.gov/article?id=Pakistan-Waste-Management> [26 April 2019]
[17] Duan Y, Huo Y and Duan L (2017). Preparation of acrylic resins modified with epoxy resins and their behaviors as binders of waterborne printing ink on plastic film. *Colloids and Surfaces A: Physicochemical and Engineering Aspects*. **535**, 225-231. https://doi.org/10.1016/j.colsurfa.2017.09.041
[18] Misra N L and Mudher K D S (2002). Total Reflection X-ray Fluorescence: A Technique for Trace Element Analysis in Materials. *Progress in Crystal Growth and Characterization of Materials*. **4**5(1-2), 65-74. https://doi.org/10.1016/S0960-8974(02)00029-3
[19] Moradllo M K, Sudbrink B, Hu Q, Aboustait M, Tabb B, Ley M T and Davis J M (2017). Using micro X-ray fluorescence to image chloride profiles in concrete. *Cement and Concrete Research*. **92**, 128-141. https://doi.org/10.1016/j.cemconres.2016.11.014
[20] Snellings R (2016). X-ray powder diffraction applied to cement. In: K. Scrivener, R. Snellings, and B. Lothenbach (eds.) *A Practical guide to microstructural analysis of cementitious materials*. CRC Press, New York. Pages 107-176.
[21] Stiegler J O and Mansur L K (1979). Radiation Effects in Structural Materials. *Annual Review of Materials Science*. **9**,405-454. https://doi.org/10.1146/annurev.ms.09.080179.002201
[22] El-Taher A (2012). Elemental analysis of granite by instrumental neutron activation analysis (INAA) and X-ray fluorescence analysis (XRF). *Applied Radiation and Isotopes*. **70**, 350–354. doi:10.1016/j.apradiso.2011.09.008
[23] Stiko R and Zawisza B (2012). *Quantification in X-Ray Fluorescence Spectrometry. In: S. K. Sharma (ed.) X-Ray Spectroscopy*, pp. 137-162. IntechOpen. Available from: http://www.intechopen.com/books/x-ray-spectroscopy/quantification-in-x-ray-fluorescence-spectrometry
[24] Karabulut Y, Canimoglu A, Kotan Z, Akyuz O and Ekdal E (2014). Luminescence of dysprosium doped strontium aluminate phosphors by codoping with manganese ion. *Journal of Alloys and Compounds*. **583**, 91–95. http://dx.doi.org/10.1016/j.jallcom.2013.08.172
[25] *ICDD Database Search - ICDD* (2019) [online] available from <http://www.icdd.com/index.php/pdfsearch> [22 April 2019]

[26] Warren B E (1940). X-ray Diffraction Study of the Structure of Glass. *Chemical Reviews*. 1940 **26** (2), 237-255. DOI: 10.1021/cr60084a007
[27] He Z H, Zhan P M, Du S G, Liu B J, Yuan W B. (2019). Creep behavior of concrete containing glass powder. *Composites Part B: Engineering*. **166**, 13-20. https://doi.org/10.1016/j.compositesb.2018.11.133.